A GEOMETRICAL ANALYSIS OF IMPACTS ON THE ISS

G.B. Valsecchi[1] and A. Rossi[2]

[1]IAS–CNR, Area della Ricerca di Roma Tor Vergata, Via Fosso del Cavaliere, 00133 Roma, Italy
[2]CNUCE–CNR, Area della Ricerca del CNR, Via Moruzzi, 1, 56100 Pisa, Italy

ABSTRACT

We use Öpik's analytical expressions that relate in a simple way the semimajor axis, eccentricity and inclination of the projectile orbit to the magnitude and direction of the relative velocity vector at impact on a given target on circular orbit, and the CODRM-94 model of debris population, to find that the large majority of the debris population is on orbits such that a correlation exists between their impact velocity on the ISS and the angle between the velocity vector of the impactor and that of the ISS.

1. ÖPIK'S VARIABLES

The space debris population can be represented in a suitable parameter space, defined with respect to the orbit of a target object on a circular orbit like the International Space Station (Valsecchi et al. 1999). This representation is based on Öpik's (1976) studies of the close approaches between small bodies and the planets, and provides useful insight into the dynamics of the overall debris population with respect to the selected target orbit.

Öpik's analytical expressions relate in a simple way the semimajor axis a, eccentricity e and inclination i of the projectile orbit to the magnitude and direction of the relative velocity vector at impact, in a reference frame that is well suited to describe the impact risk for the International Space Station (ISS).

Let us consider a target on a geocentric circular orbit of radius a_0, equatorial inclination i_0 and longitude of node Ω_0. A projectile on an orbit that actually crosses that of the target will, at the crossing point, have a velocity $\vec{U}$ relative to the target, in units of the orbital velocity of the latter, whose magnitude is equal to:

$$U = \sqrt{3 - \frac{a_0}{a} - 2\sqrt{\frac{a(1-e^2)}{a_0}}\cos I},$$

and equatorial inclination of the projectile orbit; the components of $\vec{U}$, in a frame centred on the target, with the y-axis pointing in the direction of the target's instantaneous motion and the x-axis pointing away from the Earth, are:

$$\begin{aligned} U_x &= \pm\sqrt{2 - \frac{a_0}{a} - \frac{a(1-e^2)}{a_0}} \\ U_y &= \sqrt{\frac{a(1-e^2)}{a_0}}\cos I - 1 \\ U_z &= \pm\sqrt{\frac{a(1-e^2)}{a_0}}\sin I; \end{aligned}$$

in these expressions, I is the inclination of the orbit of the projectile relative to that of the target: if the longitude of node of the projectile orbit is Ω, we have (Southworth and Hawkins 1963):

$$\sin\frac{I}{2} = \sqrt{\left[\sin\frac{i-i_0}{2}\right]^2 + \sin i_0 \sin i \left[\sin\frac{\Omega-\Omega_0}{2}\right]^2}.$$

We can introduce two useful angles, θ and ϕ, such that:

$$\begin{aligned} U_x &= U\sin\theta\sin\phi \\ U_y &= U\cos\theta \\ U_z &= U\sin\theta\cos\phi \end{aligned}$$

and, conversely:

$$\begin{aligned} \cos\theta &= \frac{U_y}{U} \\ \tan\phi &= \frac{U_x}{U_z}; \end{aligned}$$

θ is a colatitude, measured from the apex of the target motion, and ϕ is a longitude, measured from the plane containing the direction of motion of the target and the x-z plane.

Using the above formulae it is easy to derive from the orbital elements of the projectile and of the target the impact speed U, together with the two angles θ and

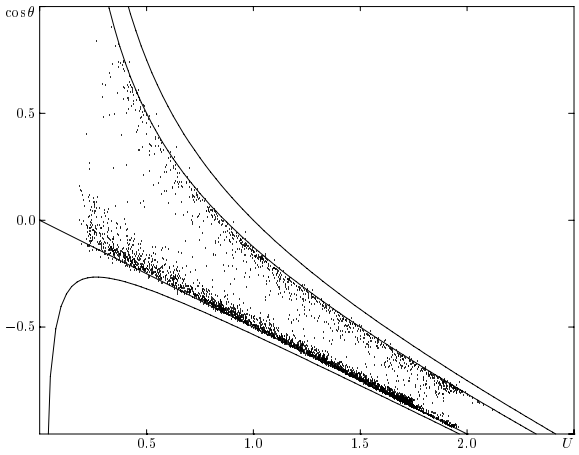

Figure 1. The CODRM-94 population of objects larger than 1 cm in the U-cosθ plane. The inclined straight line shows the condition $a = a_0$, the two curves going from top left to lower right show the condition $a = \infty$ (upper curve) and $a = 4a_0$ (lower curve), and the lowermost curve shows the condition $a = r_\oplus$ ($r_\oplus$ is the radius of the Earth); below the condition $a = a_0$ small objects are quickly removed from the population, while above the condition $a = \infty$ geocentric orbits are hyperbolic.

2. DEBRIS PARTICLE ORBITS IN THE U-COSθ PLANE

Let us now examine how a model of the current debris population of objects with diameter larger than about 1 cm, extracted from the 1994.0 CNUCE Orbital Debris Reference Model (CODRM, Pardini et al. 1996) looks like in the U-cosθ plane; this type of plot (Fig. 1) shows the relationship between collision speed and angle from the apex of the target motion. We use as target an object in an ISS-like orbit, with $a_0 = 6\,828$ km, $e = 0$, $i_0 = 52°$, $\Omega_0 = 147°$.

As it is possible to see, the debris population dos not fill all the available space between $a = r_\oplus$ and $a = \infty$, but tends to be rather concentrated close to the $a = a_0$ condition, with a secondary concentration close to the line running almost parallel to the $a = \infty$ condition, and corresponding to $a = 4a_0$; thus, from the point of view of the relationship between collision speed and angle from the apex of the target motion, the population seems to be made of essentially two components, the LEO one, with $a \approx a_0$, and the other with a much larger semimajor axis, $a \approx 4a_0$, with very little in between.

From the above considerations, we can infer that the collision speed and angle from the apex of the ISS motion are correlated. Note that each individual debris particle in the plot will change its position as time passes, due to the rotation of its nodal line relative to the nodal line of the ISS, thus changing I and therefore U; however, since the semimajor axis is not affected in this process, the point corresponding to a given particle will always remain on the curve of constant a, belonging to a family of curves whose shape can easily be inferred from those shown in the Figure and, as a consequence, the overall appearance of the Figure will not change.

3. DEBRIS PARTICLE ORBITS SEEN FROM THE ISS

Let us now consider specific ranges of U, and examine the geometry of potential impacts on the ISS. To this end, let us remark that for each set of a, e, i of the projectile orbit, there are 4 directions from which it can approach the ISS, for appropriate values of ω; these possibilities correspond to collisions taking place at the ascending or at the descending node of the orbit (relative to the ISS orbit), in the pre-perigee or post-perigee part of the orbit. Correspondingly, one can easily verify that for each set of a, e, i there is a single set of U, θ, but 4 values of ϕ, each associated to one of the possibilities listed before.

Figure 2 shows a Hammer-Aitoff (equal-area) projection of the celestial sphere, centred on the instantaneous direction of motion of the ISS, and rotating around the Earth, so that the relative longitude of the latter is $-90°$, and is marked with $\oplus$ in the diagram. As it is possible to see, for these relatively low velocities the projectiles tend to come from close to the border of the Figure, i.e. from the back, but are anyway not far from the plane perpendicular to the zenith of the ISS (the plane defined by $\sin\phi = 0$), within less than 30° of that plane.

Going to higher velocities (Fig. 3), θ increases, i.e. projectile directions move away from the back, and are confined even closer towards the plane perpendicular to the zenith. This trend continues going to still higher velocities (Figs. 4 and 5), with θ approaching (but not reaching) 180°, i.e. head-on collisions, and projectile directions concentrated closer and closer to the $\sin\phi = 0$ plane.

Figures 2, 3, 4 and 5 give an overall representation of the arrival directions of potential ISS impactors; it may be worth noting that the analytical relationships used take a negligible amount of CPU time to compute, and make the processing of very large numbers of debris particles practical.

REFERENCES

Pardini, C., Cordelli, A., Rossi, A., Anselmo, L., and Farinella P., 1996, paper AAS 95-348, Advances in the Astronautical Sciences, Astrodynamics 1995 90, 809

Öpik, E.J., 1976, Interplanetary Encounters, Elsevier, New York, USA

Southworth, R.B. and Hawkins, G.S., 1963, Smithson. Contr. Astrophys. 7, 261

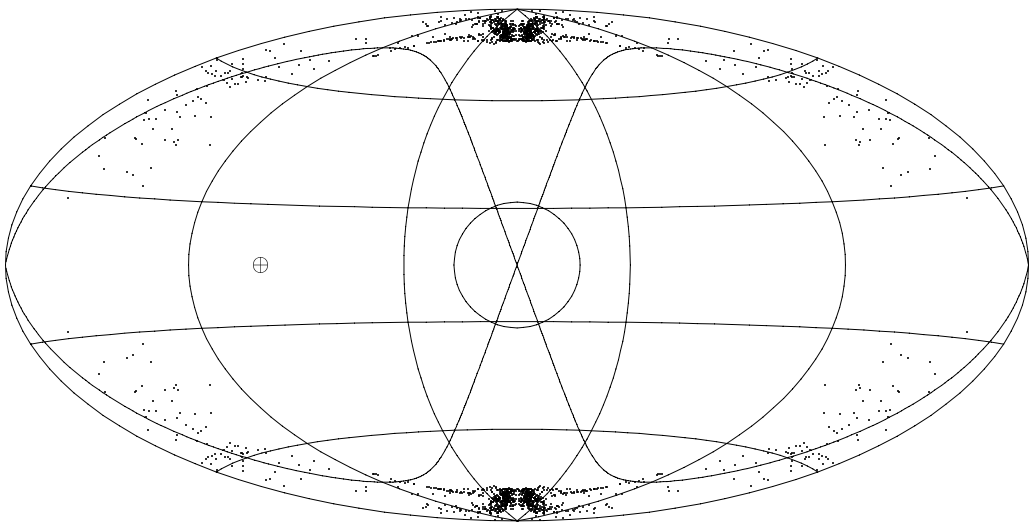

Figure 2. Hammer-Aitoff (equal-area) projection of the celestial sphere centred on the instantaneous direction of motion of the ISS, and rotating around the Earth; the latter is marked with $\oplus$ in the diagram, at longitude $\lambda - \lambda_\oplus = -90°$, latitude $B = 0°$. The centre, at $\lambda - \lambda_\oplus = 0°$, $B = 0°$, coincides with the instantaneous direction of motion of the ISS. For clarity, only the lines $\lambda - \lambda_\oplus = \pm 36°$, $\lambda - \lambda_\oplus = \pm 108°$, $B = \pm 18°$ and $B = \pm 54°$ are reported. The circle around the centre denotes $\theta = 160°$, and the four curves emanating from the centre denote (from upper right, clockwise) $\phi = 20°$, $\phi = 160°$, $\phi = 200°$, $\phi = 340°$. The dots represent members of the CODRM-94 population larger than 1 cm on orbits crossing that of the ISS, with $0 < U < 0.5$.

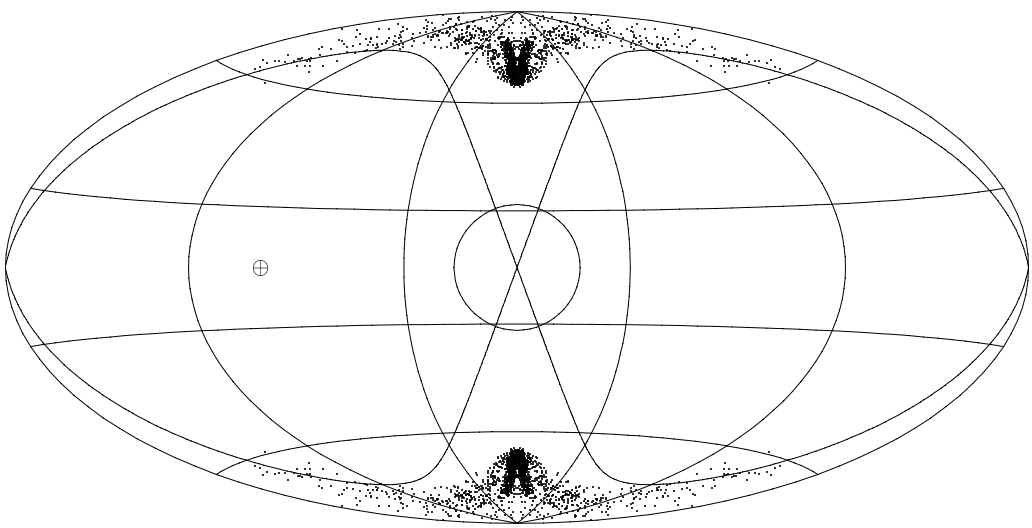

Figure 3. Same as Fig. 2, but for $0.5 < U < 1$.

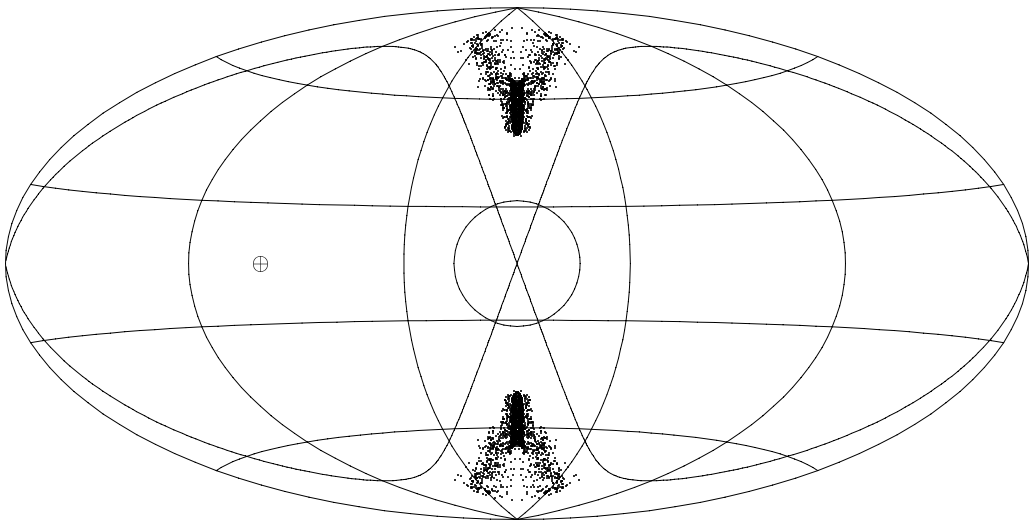

Figure 4. Same as Fig. 2, but for $1 < U < 1.5$.

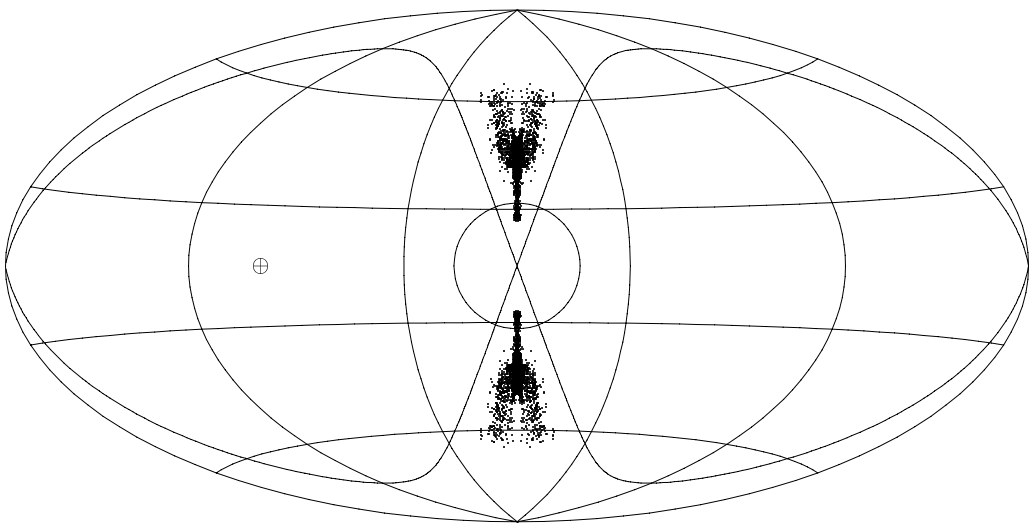

Figure 5. Same as Fig. 2, but for $1.5 < U$.